MIMO CHANNEL MEASUREMENTS AND ANALYSIS WITH PROTOTYPE USER DEVICES IN A 2GHz URBAN CELL

Mythri Hunukumbure
Centre for Communications Research,
University of Bristol
Bristol, BS8 1UB
U.K.
mh9159@bristol.ac.uk

Mark Beach
Centre for Communications Research,
University of Bristol
Bristol, BS8 1UB
U.K.
M.A.Beach@bristol.ac.uk

ABSTRACT

This paper describes an outdoor MIMO measurement campaign conducted in the 2GHz band employing a sounding bandwidth of 20MHz. The study aimed to compare the MIMO performance of two prototype devices with a reference dipole antenna module. The results obtained reveal a systematic blocking of one of the PDA antenna ports with the user's thumb alongside a significant reduction in the available MIMO channel capacity. The laptop MIMO enabled device was found to offer good MIMO capacity enhancement, matching the performance achieved with the dipole antennas.

I. INTRODUCTION

Air interface technologies employing Multiple-Input Multiple-Output (MIMO) signal processing techniques [1] are now regarded as a key enabler in the design of future wireless access systems. However, much of the analysis reported in the literature on the performance benefits of MIMO architectures, such as greatly enhanced spectrum efficiency, is based on simplified antenna and propagation channel simulation models. This paper complements a previous MIMO measurement campaign [2], [3] conducted using realistic antenna elements embedded within practical handheld devices at 5GHz for indoor operation, with a rigorous measurement and analysis campaign for an outdoor deployment at 2GHz.

Section II of this paper describes the candidate MIMO enabled devices employed in the measurements alongside their radiation pattern characteristics. The outdoor measurement campaign conducted with these devices is outlined in section III. The channel parameters are extracted as performance indicators for the candidate devices in section IV, with a particular emphasis on received SNR, body shadowing/ blocking effects, channel correlation and achievable MIMO capacities. Finally in section V, the conclusions and planned further analysis is presented.

II. PROTOTYPE MIMO ENABLED DEVICES

A. Candidate designs

Two multi-antenna prototype devices, a laptop and a PDA were designed as typical user devices to be employed in the measurements. A reference dipole module was also included to be treated as an ideal scenario, free from antenna spacing and orientation constraints and possible body shadowing/ blocking effects as encountered by the device antennas.

The prototype Laptop contained 4 Printed Inverted F Antennas (PIFA) fitted inside the back of the display panel. The 4 four antennas occupied the 2 upper edges of the back panel. Four linear slot antennas were embedded in the prototype PDA. This slot antenna design was originally carried out for the 5GHz measurements [2], and frequency scaled to suit this 2GHz campaign. The four reference dipole antennas were fitted onto a cycle helmet as two pairs of ±45˚ oriented dipoles in two orthogonal planes. The cycle helmet would be worn on the head by the user during the measurement campaign, while the device prototypes would be hand held. The receive antenna modules are depicted in Fig. 1.

(a) **(b)** **(c)**

Figure 1: The receiver antenna modules: (a) Laptop (b) PDA and (c) Reference dipolies

At the transmitter (base station) site, 2 dual polarized (±45˚) UMTS panel antennas were installed with 8˚ downtilt to obtain optimum coverage. The transmit antennas remained unchanged throughout the campaign.

B. Antenna characterisation

All the antenna modules were characterized with return loss, full 3D radiation patterns (measured in an anechoic chamber) and pattern correlation measurements. Only the distinct features observed for the two device antennas (Laptop and PDA) are discussed here.

The PIFA antennas used in the Laptop showed low cross polar discrimination properties. The co-polar and cross polar radiation patterns for one of the ports (port 1) in Fig. 2 reveal that the antennas were capable of capturing roughly equal amounts of power from V and H polariza-

tions. On average 58.6% of total power would be radiated (or absorbed) in the co polar mode.

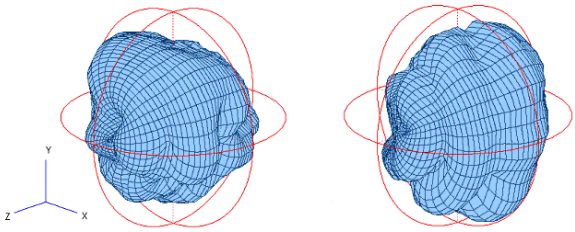

(a) **(b)**

Figure 2: **(a)** Co polar **(b)** cross polar adiation patterns for the PIFA antennas on the laptop (-40dB at Centre)

The linear slot antennas of the PDA on the other hand, retain much of the polarization purity. The co polar mode would account for 90.7% of the total radiated (or absorbed) power on average. Similar radiation patterns for the PDA antennas are given in Fig. 3 below.

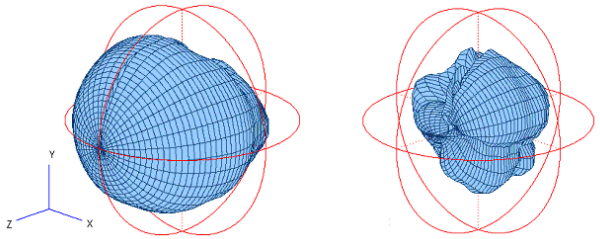

(a) **(b)**

Figure 3: **(a)** Co polar **(b)** cross polar radiation patterns for the linear slot antennas on the PDA (-40dB at Centre)

The above distinctions in the radiation patterns mark the key difference between the two device antenna designs. The other properties like the mutual coupling amongst the elements and pattern correlation are broadly similar. The dipoles arranged around the cycle helmet show equal co polar/ cross polar radiations due to the 45˚ slant, roughly making up 360˚ isotropic coverage for the combined antenna pattern.

III. The MIMO channel measurement campaign

An extensive 4x4 MIMO field trial campaign was carried out in and around the city centre of Bristol. The Medav RUSK BRI wide band channel sounder [4] was used, with 20MHz signal bandwidth centred at 2GHz carrier frequency. The base station was located on top of a 5 storey building, and the receiver equipment was taken around in a pre-planned route, while recording standing and walking measurements.

Four measurement areas, each with a cluster of measurement locations were identified for conducting the trials. Each area was covered on separate days, with the measurement route repeated for the 2 device antennas (coupled with the reference dipoles). The reference dipoles would be used immediately afterwards the device antennas. Both standing and walking (for 6m distances) mode measurements were recorded for all receive antenna modules. There were 58 measurement locations in total, and each location contained 18 measurement files from the 3 antenna modules. A channel data file would contain 4096 MIMO snapshots (instantaneous channel realizations), spanning 6.3s. The parameter settings allowed 4 MIMO snapshots to be completed within the minimum expected channel coherence time [5]. The virtual Signal to Noise ratio (SNR) could be improved by averaging these snapshots together. Fig. 4 and Fig. 5 illustrate the measurement areas/ locations and a typical measurement scenario respectively.

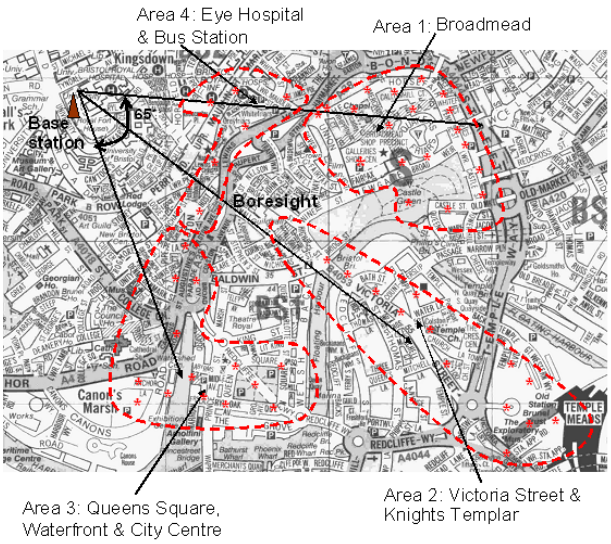

Figure 4: Map of the measurement areas and locations

Figure 5: A measurement scenario with the dipoles and prototype PDA

The measurement campaign spanned for 2 months of summer 2005. At the completion of the trials, 1053 channel data files had been recorded, which filled up 140GB of disk space.

IV. COMPARISON OF ANTENNA PERFORMANCE

The channel data was post processed to yield critical channel parameters like the average SNR, channel correlations, achievable MIMO capacity and the dynamics of the spatial eigen modes for each of the individual data files. The results from all the data files for different antenna modules have been pooled together and expressed as Cumulative Distribution Functions (CDF), to identify the general trends each antenna module would exhibit.

A. User shadowing/ blocking effects

In order to identify any user shadowing or blocking effects, the SNR values at the receiver have been estimated. The 4 snapshots collected within the channel coherence time have been used in these estimations. Without any noise addition the 4 channel responses could be considered as identical. Any variations can be attributed to the addition of Gaussian noise. The 'noise free' channel responses, y_{av}, are generated by averaging the 4 snapshots together, as shown in (1) below.

$$y_{av} = \frac{1}{4}\sum_{i=1}^{4}\sum_{j=1}^{128} x(t,\tau_j) + n(t_i,\tau_j) \quad . \qquad (1)$$

Here t and τ represent the indices in time and delay domains respectively. The signal component $x(t, \tau_i)$ is assumed to be static across the 4 snapshots. The channel responses are converted to the delay domain and the significant impulses (upto 25 dB from peak power level) of the averaged channel yield the signal power. The noise power is calculated by taking the variance across the 4 snapshots. The SNR values from the 1024 snapshot blocks and the 16 SISO sub-channels have been averaged to yield a representative value for each data file.

The SNR variations are plotted as CDFs for the 3 antenna modules in Fig. 6. The reference antennas are considered as two cases, as they were used with the PDA and the Laptop modules separately.

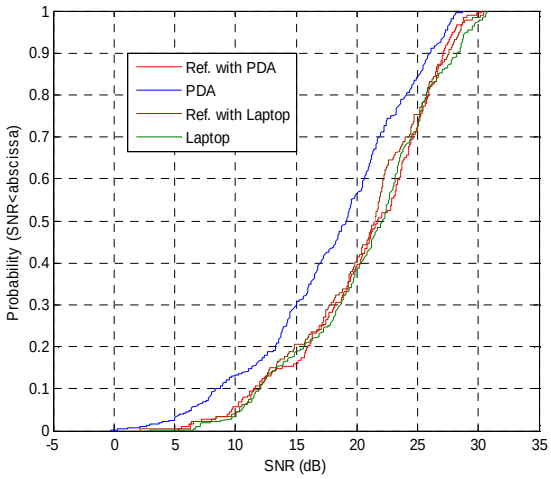

Figure 6: CDFs for SNR variations

The SNR distributions for the reference antennas with PDA and Laptop and the Laptop device antennas are broadly similar, with a median of around 22dB. However, the SNR values for the PDA device antennas are significantly lower. The difference at the median level is about 3dB. The consistently lower SNR was resulting from a particular user action. When the PDA was hand held for measurements, there was a high likelihood of the slot antenna connected to port 2 of the receiver input getting covered by the user's thumb. This action was purely unintentional on the part of the user and was identified only during post processing.

The level of impact of this blocking action can be better illustrated by plotting the CDFs of dynamic SNR ranges, as illustrated in Fig. 7. The dynamic SNR ranges were calculated from the 16 instantaneous SNR readings available for each of the sub-channels. The difference between maximum and minimum reading would represent the dynamic range. As with the SNR, dynamic ranges have been averaged across the 1024 snapshot blocks.

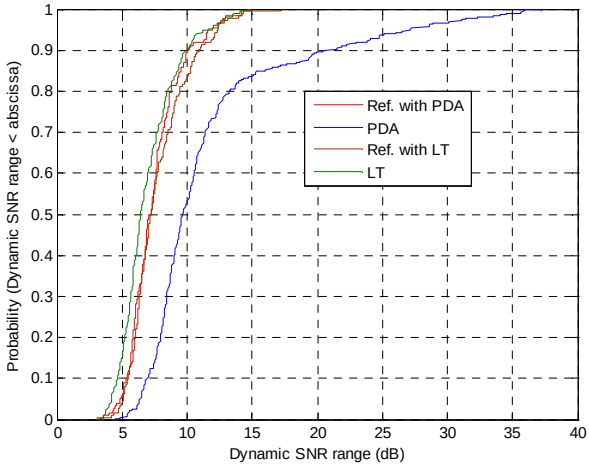

Figure 7: CDFs for SNR dynamic range variations

All 3 antenna modes except the PDA antennas have shown dynamic ranges of below 18dB. For the PDA antennas however, 90% of the cases had 20dB or below dynamic ranges and the remaining 10% varied from 20dB to 36dB. These huge increases are caused by some SISO channels having arbitrarily low reception, due to the covering of antenna port 2. Such arbitrary blocking effects would seriously undermine the performance of channel estimation and power control algorithms operated at the receiver, in a practical radio system.

In contrast, the laptop antenna module has achieved SNR levels compatible with the reference dipoles. For a small number of high end SNR (above 27dB) cases, the laptop antennas perform even better than the dipoles. High SNR values are more likely to result from LOS measurements. The transmit ports use ±45˚ polarizations, which will not be significantly altered in LOS channels. The PIFA antennas used in the laptop show very low polarization discrimination (Fig. 2) and captures equal amounts of power from both polarization modes. This property has also helped the laptop antennas to achieve more equal power distributions (lowest dynamic SNR ranges in Fig.

7). The laptop antennas here even exceed the performance of reference dipole antennas.

B. Variations in channel correlation

One of the primary targets in MIMO antenna design is to achieve sufficient de-correlation amongst the sub-channels. The recorded channel data would contain the combined effects of the radio channel and the antenna facets. However, the general trends in antenna performance could still be identified as the same measurement locations were covered by all the antennas.

The correlation co-efficient $\rho(a,b)$ between two vectors $\boldsymbol{a}$ and $\boldsymbol{b}$ could be written as;

$$\rho(a,b) = \frac{E[\boldsymbol{a}.\boldsymbol{b}^*]}{\sqrt{E[\boldsymbol{a}.\boldsymbol{a}^*].E[\boldsymbol{b}.\boldsymbol{b}^*]}} \quad . \qquad (2)$$

An essential pre-requisite for the above calculation is that both $\boldsymbol{a}$ and $\boldsymbol{b}$ should exhibit wide sense stationarity [6]. In order to avoid mean signal variations (especially in walking measurements), the channel data across the 128 frequency fingers (spanning the full 20MHz) and only 10 snapshots (spanning only 1% of measurement time) were taken to formulate $\boldsymbol{a}$ and $\boldsymbol{b}$ vectors. $\rho(a,b)$ is calculated for each of the 10 snapshot segments and averaged. The 16 sub channels would formulate a 16x16 correlation matrix. A representative single value is obtained by averaging all the non-diagonal values (avoiding self correlations of value 1) in this matrix.

The correlation co-efficients from all the channel data files are assembled and displayed as CDFs in Fig. 8 below. The 4 antenna modes are considered as before.

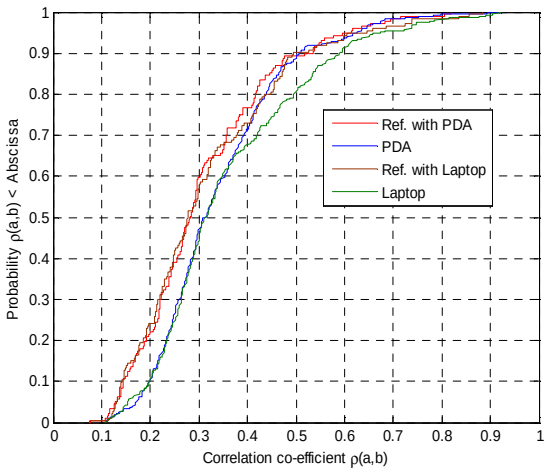

Figure 8: CDFs for channel correlations

The two reference dipole modes achieve almost identical correlation distributions with a mean value of 0.315. They are distinctly lower than the CDFs for the 2 device antenna modes, notably below $\rho(a,b)$=0.4. The lower correlations for the dipoles can be expected because of the larger inter element spacing for the dipole pairs and the orientation on different planes.

Interestingly, the PDA curve shows nearly identical correlation values as the laptop for around 65% of the data set and then crosses over to the lower correlation region of the dipoles. The PDA slot antennas show lower probability in registering high-end correlation values than the laptop PIFAs. The differences in cross polar discriminations of the two antenna types (Fig.2 and Fig. 3) do match with these observations. However the signal blocking effect on the PDA antennas could also alter the correlation calculations. Although the correlations are calculated after normalization such systematic disorders could alter the actual correlation value. Hence a clear conclusion on the correlation properties of the PDA antennas can not be drawn.

Although the laptop PIFA channel correlations do appear to be higher in the $\rho(a,b)$=[0.4-0.6] region, around 95% of measurements show correlations less than 0.7. It is only the very high correlations ($\rho(a,b)$>0.7) that significantly degrade MIMO channel capacity [7]. The PIFA antennas display superior performance in this respect, as shown in section IV(C) below.

C. Achievable MIMO capacity limits

The received SNR and the channel correlation would have a direct impact on the achievable MIMO capacity limits with these antenna modules. The achievable MIMO capacities are calculated using the fundamental information theoretic capacity limits developed by Shannon [8], and adapted for MIMO systems by Foschini and Gans [1]. The familiar 'logdet' formula for instantaneous achievable capacity (C/W) from a channel gain matrix $[H_i]n_R x n_T$, is slightly modified to account for the wideband nature of the measured data. For the wideband system, the achievable narrowband capacities over N frequency fingers are averaged across the bandwidth.

$$C/W = \frac{1}{N}\sum_{i=1}^{N}\log_2\left[\det\left(I_n + \frac{\rho}{n_T} H_i^H H_i\right)\right] \quad bits/s/Hz \qquad (3)$$

Where the received SNR is denoted by ρ and I_n is the nxn (n = min$\{n_T,n_R\}$) identity matrix. $[]^H$ stands for the Hermitian transpose.

The co-efficients in the channel gain matrix H_i were normalized, so that the mean path loss effects are nullified. The actual received SNR values (discussed in section III(A)) are used for ρ in the calculations. The wideband 4x4 MIMO capacity limits are calculated for each of the 1024 snapshots in a measurement file. The 10% outage channel capacities are derived from these ensembles as a representative figure for each channel data file. The CDFs of the 10% outage capacity values are plotted in Fig. 9 below, again for the 4 different antenna modes.

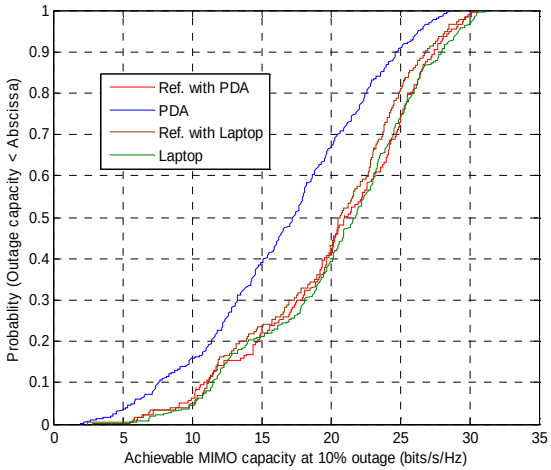

Figure 9: CDFs for 10% outage capacities

As expected, the PDA antennas give the lowest capacities, directly as a result of the reduced SNR in 4 of the 16 SISO sub-channels due to the blocking of antenna port 2. The reduction is around 4-5 bits\s\Hz, at the median level. This is a significant loss and the comparatively lower channel correlations have not been able to offset it.

The remaining antenna modes show broadly similar capacity distributions, with the CDF curves grouped together in a single cluster. A point of interest is the performance of the Laptop antennas. The slightly higher channel correlations have affected the achievable capacity limits. The higher received SNR levels these antennas achieved have even pushed the capacity levels slightly above the dipole antennas (at around 30bits/s/Hz). Hence the laptop antenna design is shown to perform well in terms of achievable MIMO capacity in an actual receiver.

V. Conclusions

This extensive channel measurement study focused on the performance of multi-antenna elements embedded within realistic prototype user devices. A key objective of the study was to identify the problems arising from the antenna spacing and orientation constraints due to the compact design of these devices and the possible user shadowing/ blocking effects. To facilitate this analysis, a reference dipole module worn at head height was also included in the measurements.

The key findings from the analysis so far have revealed a systematic blocking effect on the PDA antennas, which significantly reduces the achievable capacity limits. The PDA is a much more compact device than the laptop and its back panel would get covered by the hand when in use. This greatly reduces the options on antenna design and placement on a PDA, as all the available planes are susceptible to getting blocked by the user's hand. A viable option may be to alert the user with warning signals when such blocking occurs.

The analysis thus far has indicated that the laptop antennas (PIFA) perform well and achieve MIMO capacity levels in line with the reference dipole antennas clear of body shadowing and obstructions. The lower cross polar discrimination allows PIFAs to capture more signal power, at the cost of slightly higher channel correlation. However, the received SNR act as the overriding factor in generating significant MIMO capacity levels. The placement of the antennas in the back panel can be viewed as ideal. Not only does it prevent any blocking effects from the hands, the antennas are sufficiently far away from the user to avoid body shadowing.

Further analysis is to be carried out with the channel data to identify the dynamic behaviour of the eigen spatial modes and to observe how the antenna properties influence the rate of change in these dynamics. Also some ray tracing analysis was conducted in the same area, in order to estimate MIMO system performance and any frequency dependent characteristics when deploying MIMO enabled technology in different frequency bands.

Acknowledgements

This project was conducted under the Mobile VCE elective program and jointly sponsored by Nortel, Toshiba, Fujitsu, BT and Samsung. The authors would like to thank our sponsors for their financial backing and the numerous technical contributions to this project. Also the authors wish to thank Dr. Phill Rogers and Mr. Henry Hunt-Grubbe of CCR, Univ. of Bristol for their contributions in antenna design and pattern measurements.

References

[1] G.J. Foschini, M.J. Gans, 'On limits of wireless communication in a fading environment when using multipleantennas', Wireless Personal Communications, Vol. 6, No. 3, 1998, pp.311-335

[2] M.A. Beach, M. Hunukumbure, C. Williams, G.S. Hilton, P. Urwin-Wright, M.Capstick, 'An experimental evaluation of three candidate MIMO array designs for PDA devices', COST273, June 2004.

[3] C. Williams (editor), 'Antenna Array Technology and MIMO Systems', doc. 8366CR, deliverable to Ofcom, June 2004. available from: http://www.ofcom.org.uk/research/technology/ses/ses2003-04/ay4476b/.

[4] http://www.medav.de/index_e.html

[5] J.D. Parsons, *The mobile radio propagation channel*, 2nd Edition, Wiley, Chichester, U.K. 2000.

[6] R. Steele, L. Hanzo, *Mobile radio communications*, 2nd Edition, Chapter 2, Wiley, Chichester, U.K. 1999.

[7] B. Vucetic, J. Yuan, *Space Time Coding*, chapter 1, pp.30-49, Wiley Publishers, Chichester, U.K. 2003.

[8] C.E. Shannon, "A Mathematical theory of communication", Bell Systems Technical Journal, Vol.27, 1948, pp. 379-423 and 623-656.